# Enhancement of the Modulation Dynamics of an Optically Injection-Locked Semiconductor Laser Using Gain Lever

Jean-Maxime Sarraute, Kevin Schires, Sophie LaRochelle, *Senior Member, IEEE*, and Frédéric Grillot, *Senior Member, IEEE*

***Abstract*—The modulation response of an optically injected gain-lever semiconductor laser is studied for the first time using small-signal analysis of a rate equation model. Calculations show that a gain-lever laser operating under medium to strong optical injection provides a unique and robust configuration for ultralarge bandwidth enhancement. Modulation bandwidths above nine times the relaxation oscillation frequency of the free-running laser can be reached using injection-locking conditions that are reasonable for practical applications. This theoretical work is of prime importance for the development of directly modulated broadband optical sources for high-speed operation at 40 Gb/s and beyond.**

***Index Terms*—Semiconductor laser, bandwidth, modulation response, optical injection, gain lever.**

## I. Introduction

DIRECT modulation of semiconductor lasers at high frequencies is a major challenge in the development of low-cost fiber optic communication networks [1]. In these systems, the modulation bandwidth (in gigahertz) of a directly modulated laser (DML) is the most important figure-of-merit that determines the maximum data rate (in Gb/s) achievable. In order to improve the performance and capacity of such optical networks for operation at 40 Gb/s and above, it is necessary to first enhance the modulation efficiency and bandwidth of the optical transmitters. This must however be done without increasing their intensity noise or low-signal distortion, and without suffering from optical frequency deviation (frequency chirp). Owing to their low-cost, well-established fabrication, compactness and most importantly their efficiency, DMLs remain the most promising candidates for modulated optical sources of high-speed low-cost communication networks using intensity modulated formats with direct detection [2]. However, the bandwidth of conventional DMLs remains strongly limited by the intrinsic relaxation oscillation frequency of the laser gain medium, from a few to tens of gigahertz [3].

As an alternative, external optical modulators are generally used in order to reach larger bandwidths with a high linearity and low chirp [4]. However, this configuration greatly increases the cost and power requirements of the overall network. Operation cost and power consumption can be reduced when the laser is directly integrated with a modulator, however fabrication costs and power requirements remain higher than in the case of DMLs [3]. While simpler to implement, direct modulation involves modulating the electrical pump current around the above-threshold bias of the laser, and the light produced thus strongly depends on the nonlinear characteristics of the laser cavity dynamics. In order to improve the modulation characteristics and to cope with the fast-growing need for energy-saving and high-bandwidth laser diodes [5], [6], the control of intrinsic parameters of the device such as optical gain or confinement is highly desirable [7].

It is well-known that the modulation capabilities of DMLs are mostly limited by frequency chirp and intrinsic parasitic effects driven by nonlinear gain suppression or carrier transport delay [3]. The best performers, edge-emitting lasers, have achieved modulation bandwidths of up to 40 GHz [8], [9]. Vertical-cavity-surface-emitting lasers (VCSEL) have slightly lower records, including a 20-GHz bandwidth allowing for 25 Gb/s modulation in a 1.1 $\mu$m VCSEL [10], and 10-Gb/s modulation with a 1.55 $\mu$m VCSEL [11]. The most fundamental speed limitation in conventional DMLs is the resonance frequency, typically below 20 GHz. The fastest DMLs have resonance frequencies in the range of 5–30 GHz [8]–[11]. Over the past few years, tremendous efforts have been made to improve the modulation dynamics of semiconductor lasers. Indeed, most of the aforementioned effects can be attained using high-quality materials and optimization of the device structure. Most importantly, similar and further improvements can be achieved using nonlinear photonic techniques such as the use of optical injection-locking (OIL) [12], [13], or the use of optical gain lever (GL) architectures [14], [15].

OIL relies on the locking of a slave laser (SL) at the frequency of the light from a master laser (ML), which is directly injected into the SL cavity. Injection-locking regime is reached

Manuscript received February 6, 2015; revised April 30, 2015 and May 27, 2015; accepted June 10, 2015. This work was supported by the Institut Mines-Tlcom, the European Office of Aerospace Research and Development under Grant FA9550-15-1-0104 and by a public grant overseen by the French National Research Agency (ANR) through the Nanodesign Project supported by the IDEX Paris-Saclay, ANR-11-IDEX-0003-02. This work was also supported in part by the NSERC through the CRC in Advanced Photonics Technologies for Communications.

J.-M. Sarraute is with the Université Paris-Saclay, Télécom ParisTech, Paris 75013, France, and also with the Centre d'optique, photonique et laser, Université Laval, Québec, QC G1V 0A6, Canada (e-mail: jean-maxime.sarraute@telecom-paristech.fr).

K. Schires and F. Grillot are with the Université Paris-Saclay, Télécom ParisTech, Paris 75013, France (e-mail: kevin.schires@telecom-paristech.fr; frederic.grillot@telecom-paristech.fr).

S. LaRochelle is with the Centre d'optique, photonique et laser, Université Laval, Québec, QC G1V 0A6, Canada (e-mail: sophie.larochelle@gel.ulaval.ca).

Color versions of one or more of the figures in this paper are available online at http://ieeexplore.ieee.org.

Digital Object Identifier 10.1109/JSTQE.2015.2445876

when the strength of the injected ML light and the frequency detuning between the ML and SL fall within a certain range described below [16]. In this regime, the dynamical characteristics of the SL can be greatly improved: the injected oscillator exhibits relaxation oscillation frequencies much higher than its free-running value $f_{\mathrm{R}}$, nonlinear distortion is suppressed, relative intensity noise is lowered, and spectral characteristics such as mode hopping, frequency chirp and linewidth are reduced [17]–[21]. However, strong optical injection is often crucial for reaching the ultimate limits of modulation bandwidth enhancement in injection-locked lasers [22]. Under strong optical injection, a beating between the injected light frequency and the cavity resonant frequency dominates the dynamic behavior and controls an enhanced resonance in the modulation response of the locked laser. Obtaining the widest possible stable locking range in terms of frequency detuning thus allows reaching a resonance at very high frequencies. The highest excitation of the modulation dynamics experimentally observed reached a relaxation frequency beyond 100 GHz and a 3-dB bandwidth of 80 GHz by far exceeding those achieved for free-running devices. These results have been reported both for injection-locked VCSELs and DFB lasers [13]. Nevertheless, it is important to note that while the relaxation oscillation frequency increases with the injected power, the modulation bandwidth can in fact be lower than in the free-running case due to a frequency dip arising in the modulation response of the SL [23]. To this end, recent results have shown the possibility to maintain a relative broadband and flat modulation response by controlling both the differential gain and the linewidth enhancement factor of a quantum dash Fabry–Perot laser, operating under strong optical injection [24]. However, further enhancements of injection efficiency remain difficult to reach as both a low mirror reflectivity and a short cavity roundtrip times are required in order to maximize the coupling of the injected light into the SL cavity. In edge-emitting lasers, the beneficial effect of a rather low mirror reflectivity on the injection coupling coefficient is counteracted by a large cavity roundtrip time resulting from the long laser cavity. Similarly, even though optically-injected VCSELs benefit greatly from very short cavities, and hence very small cavity roundtrip time, their high-speed performances are compromised by a very high mirror reflectivity resulting in coupling rate coefficients similar to that of edge emitters. In addition, VCSELs pose a very challenging alignment problem in injection-locking experiments and, at the same time, are not suitable for monolithic integration of the ML and SL.

In contrast, GL takes advantage of the sublinear relationship between optical gain and pump current in a semiconductor laser, due to the optical gain saturation occurring with increasing carrier density. Assuming a single-section laser (no optical interface within the cavity) with two coupled electrical sections, the modulation efficiency can be increased by using radio-frequency (RF) modulation on only one of the electrical sections, continuous-wave (CW) biased below the lasing threshold such that its differential gain is substantially higher than in the case of a laser biased well above its threshold. The GL photonic chip thus provides a monolithic way to improve and shape the modulation performance of semiconductor lasers with little impact on $f_{\mathrm{R}}$ and without any requirement on the optical properties of the laser, hence requiring little modification of its design and fabrication [14], [15], [25]. For instance, in [26] a 6 dB enhancement of the amplitude modulation efficiency was reported using an optical GL quantum well (QW) device. A 22 dB modulation efficiency increase was also realized using a 220-$\mu$m QW laser, with only a marginal increase in the intensity noise [25]. Recent results have also reported that the strong gain saturation in quantum dot (QD) lasers operating with GL effect can be beneficial for enhancing the 3-dB bandwidth at least by a factor of three as compared to the uniform bias condition [27], [28]. Such enhancements of the modulation efficiency with little effect on $f_{\mathrm{R}}$ thus promises increased modulation bandwidths in GL DMLs. Unfortunately, because the improved amplitude modulation efficiency is achieved at the expense of linearity in the gain versus injection current curve, a major drawback of GL lasers is the increase of non-linear distortion.

The combination of both effects represents a promising configuration where the drawbacks of OIL and GL balance each other, potentially leading to DMLs with much larger modulation bandwidths and a rather flat modulation response. To the best of our knowledge, only a single experimental study has reported on an injection-locked GL DFB, showing a 10 dB increase of modulation efficiency and a three times enhanced modulation bandwidth, associated to a suppression of the third-order intermodulation distortion [29]. Furthermore, the improvement of the dynamic characteristics of the OIL laser such as the reduction of its linewidth may in addition reduce the impact of effects such as frequency chirp, but little substantiated studies have been done on this topic.

This paper presents the first theoretical investigation of an optically injection-locked gain-lever (OILGL) laser. Using small-signal analysis of a comprehensive semi-analytical model based on a set of differential rate equations, a novel expression of the transfer function of the OILGL is derived. The modulation properties are then investigated as a function of the OIL and GL parameters. The paper is organized as follows. In Section II, the theoretical model describing the OILGL is presented. From a small-signal analysis of the differential rate equations, the transfer function of the OILGL laser is introduced. In Section III, simulations are discussed and key-features driving the modulation properties are emphasized. Numerical results are first studied in cases where only either GL or optical injection is used, and is compared to previous theoretical work. When studying the combination of both effects, calculations reveal that a GL laser operating under medium to strong optical injection provides a unique configuration for ultra-large bandwidth enhancement. Finally, we summarize our results and conclusions in Section IV.

## II. Rate Equations for Optically-Injected Semiconductor GL Lasers

Fig. 1(a) shows a schematic view of the GL laser and the evolution of the gain with the carrier density in the semiconductor

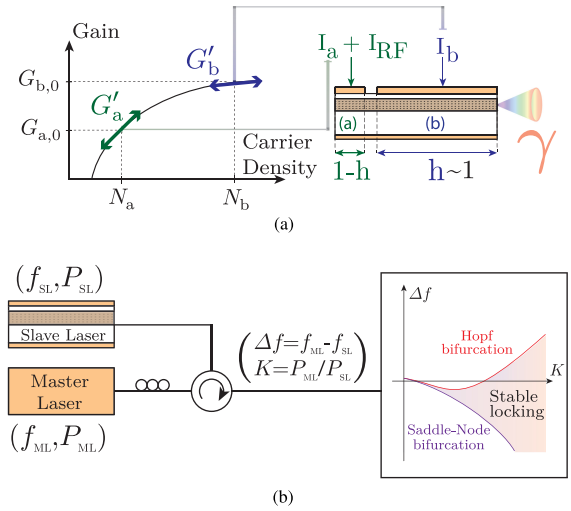


Fig. 1. (a) Schema of the GL laser; The right figure gives the evolution of the material gain with carrier density and shows the differential gain in both sections; (b) Schematic view of the equivalent setup for optical injection of the GL laser. The right figure represents the injection locking map and its boundaries.

material. Section (a), the modulation section, is very short and biased at $I_a + I_{RF}$, close to optical transparency (with a material gain $G_{a,0} \simeq 0$). Section (b), the gain section, is CW-biased at $I_b$ and pumped well above the lasing threshold, and its fractional length $h$ is taken close to unity. Section (b) thus provides a higher material gain that is clamped to its value at threshold ($G_{b,0} \simeq G_{th}$) and balances the optical cavity losses. The differential gain of section (a) is thus much higher than that of section (b) ($G'_a \gg G'_b$), hence any small change in carrier density induced by current modulation in this section induces a larger variation in carrier density in the gain section and consequently in the total number of photons. In other words, it is possible to obtain a very large change in carrier density in the gain section driven above threshold, using only a small variation of current in the modulation section.

Fig. 1(b) depicts a schematic view of the OILGL laser. OIL of semiconductor lasers involves two optical sources, referred to as the ML and SL. The light output from the ML, typically a single-mode narrow-linewidth tunable laser, is injected into the SL cavity. The two degrees of freedom of optical injection of edge-emitting semiconductor lasers are the frequency detuning between the ML and SL $\Delta f = f_{ML} - f_{SL}$, with $f_{ML/SL}$ the lasing frequency of the ML/SL, and the injected power $P_{ML}$. These scale to the characteristics of the free-running SL, namely its relaxation oscillation frequency $f_R$ and its output power $P_{SL}$. The ratios $\Delta f/f_{RF}$ and $K = P_{ML}/P_{SL}$ are thus commonly used to indicate the optical injection conditions, and allow comparison between results obtained with different lasers. Within the stable injection-locking regime, the SL wavelength is locked onto the injected ML wavelength. As shown on the right hand side of Fig. 1(b), the stable-locking area is limited by two types of bifurcations: a Hopf bifurcation in the upper part of the locking region and a saddle-node bifurcation in its bottom part [30]. The asymmetry between these two bifurcations mainly depends on the linewidth enhancement factor of the semiconductor laser [16].

The analysis of the OILGL semiconductor laser can be described through a comprehensive set of differential rate equations:

$$\begin{cases} \dfrac{dN_{e^-,a}}{dt} = \dfrac{J_a}{eD} - \dfrac{N_{e^-,a}}{\tau_{c,a}} - G_a N_\gamma & \text{(1a)} \\ \dfrac{dN_{e^-,b}}{dt} = \dfrac{J_b}{eD} - \dfrac{N_{e^-,b}}{\tau_{c,b}} - G_b N_\gamma & \text{(1b)} \\ \dfrac{dN_\gamma}{dt} = \mathcal{F} N_\gamma + 2k_c\sqrt{N_{\gamma,inj} N_\gamma}\cos(\phi) & \text{(1c)} \\ \dfrac{d\phi}{dt} = \dfrac{\mathcal{F}\alpha_H}{2} - \Delta\omega_{inj} - k_c\sqrt{\dfrac{N_{\gamma,inj}}{N_\gamma}}\sin(\phi) & \text{(1d)} \end{cases}$$

where $N_{e^-,k}$ is the carrier density of section $k$, $J_k$ its current density, $\tau_{c,k}$ the carrier lifetime and $G_k$ the optical gain. In addition, $N_\gamma$ and $\tau_p$ are the photon density and lifetime, respectively, of the SL cavity of linewidth enhancement factor $\alpha_H$. According to [3] a logarithmic gain is taken into account such that:

$$G_k(N_{e^-,k}, N_\gamma) = \frac{G_{k,0}}{1+\varepsilon N_\gamma} \ln\left(\frac{N_{e^-,k} + N_s}{N_{tr} + N_s}\right) \quad (2)$$

where $\varepsilon$ is the gain compression factor, $N_{tr}$ is the carrier density at the transparency and $N_s$ is a fitting parameter that is used to force the natural logarithm to be finite at $N_{e^-,k} = 0$ [3]. Regarding the optical injection, $N_{\gamma,inj}$ is the photon density injected with a coupling factor $k_c$ and detuned from the free-running SL by $\Delta\omega_{inj} = 2\pi\Delta f$, with $\phi$ the phase offset between ML and SL. Finally $\mathcal{F}$ corresponds to $\mathcal{F} = \Gamma\left[G_a(1-h) + G_b h\right] - \dfrac{1}{\tau_p}$ where $h$ is the fractional length of section (b) and $\Gamma$ the optical confinement factor.

As in [27], spontaneous emission is ignored in (1a) and (1b) and the same photon density and phase evolution is assumed in (1c) and (1d) as in [31].

In analogue modulation, a sinusoidal current variation is usually added to the continuous bias current. The modulation response of a semiconductor laser is thus studied by solving the rate equations with a time-varying current $I(t) = I_1 + i_m e^{j\omega t}$, where $I_1$ is the bias current and $i_m$ the modulation current. Analytic solutions of the rate equations can simply be obtained by biasing the laser above threshold such that $I_1$ is larger than the threshold current $I_{th}$, with $i_m << I_1 - I_{th}$. This small-signal condition leads to variations of carrier density $N_{e^-}$ and output power $P$ well below the steady-state values $N_{th}$ and $P_0$, respectively. It is therefore possible to linearize the rate equations and solve them analytically using the Fourier transform technique [32]. In our configuration, a small-signal analysis of the rate equations is used to derive the transfer function of the OILGL laser by considering $J_k$, $G_k$, $N_{e^-,k}$, $N_\gamma$ and $\phi$ as dynamical variables. In order to do so, let us assume solutions of the form:

$$\begin{cases} dX = X_1 e^{\imath\omega t} & \text{(3a)} \\ dG_k = \dfrac{G'_{k,0}}{1+\varepsilon N_\gamma} dN_{e^-,k} - \dfrac{\varepsilon G_k}{1+\varepsilon N_\gamma} dN_\gamma & \text{(3b)} \end{cases}$$

where $X$ can be any variable other than the optical gain. Relation (3b) comes from the derivation of equation (2) with respect to $N_\gamma$ and $N_{\mathrm{e^-,k}}$, where the differential gain $G'_{\mathrm{k},0}$ is defined as $G'_{\mathrm{k},0} = \partial G_k / \partial N_{\mathrm{e^-,k}} = G_{\mathrm{k},0} / \left(N_{\mathrm{e^-,k}} + N_{\mathrm{s}}\right)$. In what follows, the gain compression factor is not taken into account ($\varepsilon = 0$) and its impact on the OILGL modulation dynamics is left over for further studies. Combining (3) into the differential rate equations leads to:

$$\begin{bmatrix} m_{11} & 0 & m_{13} & 0 \\ 0 & m_{22} & m_{23} & 0 \\ m_{31} & m_{32} & m_{33} & m_{43} \\ m_{41} & m_{42} & m_{43} & m_{44} \end{bmatrix} \begin{bmatrix} N_{e^-,a,1} \\ N_{e^-,b,1} \\ N_{\gamma,1} \\ \phi_1 \end{bmatrix} = \begin{bmatrix} J_{\mathrm{a},1}/\mathrm{eD} \\ J_{\mathrm{b},1}/\mathrm{eD} \\ 0 \\ 0 \end{bmatrix} \tag{4}$$

with

$$\begin{aligned} m_{11} &= \imath\omega + \frac{1}{\tau_{\mathrm{c,a}}} + G'_{\mathrm{a},0} N_\gamma, & m_{13} &= \frac{1}{\tau_{\mathrm{p}}} - G_{\mathrm{a},0} N_\gamma \\ m_{22} &= \imath\omega + \frac{1}{\tau_{\mathrm{c,b}}} + G'_{\mathrm{b},0} N_\gamma, & m_{23} &= \frac{1}{\tau_{\mathrm{p}}} - G_{\mathrm{b},0} N_\gamma \\ m_{31} &= -\Gamma(1-h) G'_{\mathrm{a},0} N_\gamma, & m_{32} &= -\Gamma h G'_{\mathrm{b},0} N_\gamma \\ m_{33} &= \imath\omega + \eta\cos(\phi_1), & m_{34} &= 2\eta N_\gamma \sin(\phi_1) \\ m_{41} &= -\frac{\alpha_{\mathrm{H}}\Gamma(1-h) G'_{\mathrm{a},0}}{2}, & m_{42} &= -\frac{\alpha_{\mathrm{H}}\Gamma h G'_{\mathrm{b},0}}{2} \\ m_{43} &= -\frac{1}{2N_\gamma}\eta\sin(\phi_1), & m_{44} &= \imath\omega + \eta\cos(\phi_1) \end{aligned} \tag{5}$$

where $m_{33}$ and $m_{44}$ are coefficients given by the steady state solution of (1c) and (1d). Let us note that $\eta$ is expressed as follows:

$$\eta = k_{\mathrm{c}} \sqrt{\frac{N_{\gamma,\mathrm{inj}}}{N_\gamma}} = k_{\mathrm{c}} \sqrt{K}. \tag{6}$$

The photon lifetime and internal losses are given by $\tau_{\mathrm{p}} = n_{\mathrm{g}} / \left[c\left(\alpha_{\mathrm{i}} + \alpha_{\mathrm{m}}\right)\right]$ and $\alpha_{\mathrm{m}} = -\ln(R)/L$ while the coupling factor $k_{\mathrm{c}}$ depends on $R$, $L$ and $n_{\mathrm{g}}$ following:

$$k_{\mathrm{c}} = \frac{c\left(1-R\right)}{2 n_{\mathrm{g}} L \sqrt{R}}. \tag{7}$$

Then, the extraction of the modulation transfer function $\mathfrak{R}\left(\omega\right) = N_{\gamma,1}(\omega)/J_{\mathrm{a},0}(\omega)$ is performed using Cramer's rules to express $N_{\gamma,1}$ as the following determinant quotient,

$$N_{\gamma,1} = \frac{\begin{vmatrix} m_{11} & 0 & J_{\mathrm{a},1}/\mathrm{eD} & 0 \\ 0 & m_{22} & J_{\mathrm{b},1}/\mathrm{eD} & 0 \\ m_{31} & m_{32} & 0 & m_{43} \\ m_{41} & m_{42} & 0 & m_{44} \end{vmatrix}}{\begin{vmatrix} m_{11} & 0 & m_{13} & 0 \\ 0 & m_{22} & m_{23} & 0 \\ m_{31} & m_{32} & m_{33} & m_{43} \\ m_{41} & m_{42} & m_{43} & m_{44} \end{vmatrix}}. \tag{8}$$

Assuming $h \sim 1$ and $J_{\mathrm{b}} \gg J_{\mathrm{a}}$, the normalized modulation transfer function of the OILGL laser $R(f) = \mathfrak{R}(f)/\mathfrak{R}(0)$ can be expressed as follows:

$$|R(f)|^2 = \frac{\mathcal{A}_0^2 \left[\left(\eta - \mathcal{A}'_2 f^2\right)^2 + \left(\mathcal{A}'_1 f\right)^2\right]}{\left[\mathcal{A}_1 f - \mathcal{A}_3 f^3\right]^2 + \left[\eta\mathcal{A}_0 - \mathcal{A}_2 f^2 + f^4\right]^2}. \tag{9}$$

Equation (9) constitutes a novel expression of the modulation transfer function describing an OILGL, in which all parameters $A_{\mathrm{i}}$ correspond to:

$$\begin{aligned} \mathcal{A}_0 &= \frac{\eta\gamma_{\mathrm{b}}^2 g}{16\pi^4} + \frac{\gamma_{\mathrm{b}} g \mathfrak{Z}_{\phi,\alpha_{\mathrm{H}}} \sigma}{16\pi^4},\ \mathcal{A}'_1 = \frac{2\pi}{\mathfrak{Z}_{\phi,\alpha_{\mathrm{H}}}} + \frac{2\pi\eta}{\gamma_{\mathrm{b}}} \\ \mathcal{A}_1 &= \left[\gamma_{\mathrm{b}}\left(g+1\right)\eta^2 + 2\eta\cos(\phi)\gamma_{\mathrm{b}}^2 g + \sigma\left(\gamma_{\mathrm{b}} g\right.\right. \\ &\quad \left.\left. +\ \eta\mathfrak{Z}_{\phi,\alpha_{\mathrm{H}}}\right)\right] \frac{1}{8\pi^3}, \\ \mathcal{A}_2 &= \left[\eta^2 + 2\eta\cos(\phi)\gamma_{\mathrm{b}}\left(g+1\right) + \gamma_{\mathrm{b}}^2 g + \sigma\right] \frac{1}{4\pi^2}, \\ \mathcal{A}'_2 &= \frac{4\pi^2}{\gamma_{\mathrm{b}}\mathfrak{Z}_{\phi,\alpha_{\mathrm{H}}}}, \qquad \mathcal{A}_3 = \left[2\eta\cos(\phi) + \gamma_{\mathrm{b}}\left(g+1\right)\right] \frac{1}{2\pi} \end{aligned} \tag{10}$$

with $\sigma$ and $\mathfrak{Z}_{\phi,\alpha_{\mathrm{H}}}$ defined as:

$$\sigma = \frac{1}{\tau_{\mathrm{p,slave}}}\left(\gamma_{\mathrm{b}} - \frac{1}{\tau_{\mathrm{c,b}}}\right), \quad \mathfrak{Z}_{\phi,\alpha_{\mathrm{H}}} = \cos(\phi) - \alpha_{\mathrm{H}}\sin(\phi). \tag{11}$$

Finally, let us note that $g$ is expressed as follows:

$$g = \frac{\gamma_{\mathrm{a}}}{\gamma_{\mathrm{b}}}, \tag{12}$$

where $\gamma_{\mathrm{a}}$ and $\gamma_{\mathrm{b}}$ are the damping rate factors for sections (a) and (b), respectively. Let us stress that these two different damping rates are included to describe the damping effect on the resonance frequency and the modulation response. These are related to the carrier lifetime, photon density and differential gain [27]. It is also important to emphasize that $(\gamma_{\mathrm{b}}, g)$ are the parameters representing the GL effect while $(\Delta\omega_{\mathrm{inj}}, K)$ are those controlling the optical injection conditions. In order to obtain a strong GL effect, the device operation point is chosen such that the resultant differential gain ratio $G'_{\mathrm{a}}/G'_{\mathrm{b}}$ is as large as possible, which is obtained by pumping the short section close to optical transparency and the longer one above the lasing threshold. Under these conditions, the ratio of the damping rates quantifies the strength of the GL effect.

The detuning coefficient $\Delta\omega_{\mathrm{inj}}$ is related to the phase shift $\phi$ and the frequency detuning $\Delta f$ by the relations :

$$\Delta\omega_{\mathrm{inj}} = 2\pi\Delta f, \quad \phi = \arcsin\left[-\frac{\Delta\omega_{\mathrm{inj}}}{\eta\sqrt{\alpha_{\mathrm{H}}^2+1}}\right] - \tan^{-1}\left(\alpha_{\mathrm{H}}\right). \tag{13}$$

The next section investigates the different configurations where these key parameters are varied first independently to study their respective effects, then together.

TABLE I
MATERIAL AND LASER PARAMETERS

| Simulation parameters | Symbols | Value |
|---|---|---|
| Cavity length | $L$ | $500 \times 10^{-6}$ m |
| Mirror reflectivity | $R_1 = R_2$ | 0.32 |
| Internal modal losses | $\alpha_{\mathrm{i}}$ | $14 \times 10^{2}$ m$^{-1}$ |
| Mirror losses | $\alpha_{\mathrm{m}}$ | $22.8 \times 10^{2}$ m$^{-1}$ |
| Optical index | $n_{\mathrm{g}}$ | 3.5 |
| Carrier lifetime | $\tau_{\mathrm{c}}$ | $0.1 \times 10^{-9}$ s |
| Photon lifetime | $\tau_{\mathrm{p}}$ | $3.17 \times 10^{-12}$ s |
| Linewidth Enhancement Factor | $\alpha_{\mathrm{H}}$ | 2 |
| Coupling S-M factor | $k_{\mathrm{c}}$ | $1 \times 10^{11}$ s$^{-1}$ |
| Damping rate factor (section b) | $\gamma_{\mathrm{b}}$ | 12, 20 GHz |

## III. RESULTS AND DISCUSSION

All material and laser parameters used in the calculations are given in Table I and correspond to an InAs/InP QD laser structure with lasing wavelength around 1550 nm, the study being performed in a similar fashion as in [27]. Although the model does not fully take into account the fine structure of a QD laser [33], [34], the basic features of the nanostructures are implicitly incorporated into the rate equations through the set of parameters reported in Table I.

### A. Free-Running GL

In this section, the GL laser is studied without optical injection ($K = 0$ and $\phi = -\pi/2$). Let us note that while the terms using $\phi$ disappear in the rate equations, the terms $A_0$, $A_1'$ and $A_2'$ of the transfer function do still depend on $\phi$. To this end, a value of $-\pi/2$ is used to obtain an expression of these terms similar to the free-running model.

The description of the GL laser usually requires two damping rates that are related to the different carrier dynamics introduced by the asymmetric pumping. Specifically, the modulation efficiency enhancement is known to be directly proportional to the ratio of the differential gains of the two sections [27]. This study concentrates on a limiting case such that $G_{\mathrm{a},0} = 0$ and $h \approx 1$, in other words a very short modulation section biased close to optical transparency. Therefore, the gain section accounting for the majority of the device, both the damping rate and relaxation oscillation frequency $f_{\mathrm{R}}$ of the gain section are approximated to that of the uniformly-biased device. Fig. 2 depicts the modulation response calculated for $g = 1$, 2, 4 and 10. In Fig. 2, the $x$-axis is normalized to the free-running $f_{\mathrm{R}}$ in order to express the bandwidth enhancement in a way that is not device-specific. Solid lines are directly calculated from (9) while the superimposed white dashed lines show the results obtained using the original modulation transfer function of the GL laser from [27]. Very good agreement is thus found between this previous formulation of the GL effect and our novel transfer function (9). In what follows, a damping rate of the gain section $\gamma_{\mathrm{b}}$ of 12 GHz is used in order to obtain realistic pumping conditions of the laser. Under these conditions the free-running relaxation oscillation frequency $f_{\mathrm{R}}$ is of 3.8 GHz. The red solid line is obtained under uniform pumping conditions ($g = 1$, no GL effect). As already described in [27], the $-3$ dB modulation bandwidth $f_{-3\mathrm{dB}}$ is found to be limited to 1.55 $\times f_{\mathrm{R}} \approx 6$ GHz [33]. These results are well known for QD lasers for which $f_{\mathrm{R}}$ is limited by the maximum material gain and gain compression effects, while the strong damping factor of such lasers limits $f_{-3\mathrm{dB}}$ [35]. As $g$ is increased beyond the unity, i.e., by moving from uniform to asymmetric pumping conditions, simulations reveal the GL effect. The amplitude of the modulation response is largely increased with little effect on the relaxation oscillation frequency even under a strong asymmetric bias ($g = 10$). In addition, for $f > f_{\mathrm{R}}$, the slope of the transfer functions is slightly reduced with increasing values of $g$. These two effects combined allow a large increase of the $-3$ dB modulation bandwidth for the GL laser. For instance, a free-running GL device operating with $g$ =10 would exhibit values of $f_{-3\mathrm{dB}}$ of about 3 $\times f_{\mathrm{R}} \approx 11$ GHz. The latter corresponds to an increase of $f_{-3\mathrm{dB}}$ by factor of two compared to the case $g = 1$. However, the enhancement of the modulation efficiency (increasing by about 5 dB in Fig. 2 around $f = f_{\mathrm{R}}$) may lead to a larger non-linear distortion, and is the main drawback of the GL.

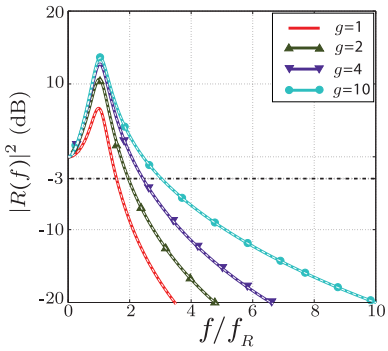


Fig. 2. Transfer functions of the free-running GL laser calculated for $g = \{1, 2, 4, 10\}$ both from (9) (solid lines and markers) with $K = 0$ and $\phi = -\pi/2$, and from the classical GL model (superimposed white dashed lines).

### B. Optical Injection-Locking

In this section transfer functions are now calculated from (9) without GL effect ($g = 1$) in the case of optical injection only. Fig. 3 depicts modulation responses calculated for various values of the injection strength $K$. For each value of $K$, the frequency detuning $\Delta f$ is chosen so that the SL is operated within the stable locking range very close to the Hopf bifurcation in order to better see the resonance in the modulation response [30]. For the studied range of injection strengths, $K$ = 0 (free-running), 0.5, 2 and 5, the corresponding values of the normalized detuning are thus $\Delta f/f_{\mathrm{R}} = 0$, $-2.20$, 1.12 and 6.10. Fig. 3(a) shows that the injection-locking configuration greatly increases the resonance frequency up to a value of 9 times the free-running $f_{\mathrm{R}}$ for $K = 5$. This large enhancement mostly results from the beating between the ML light frequency and the cavity resonant frequency. Note that these are not detuned by $\Delta f$ anymore when $K$ becomes large as the SL cavity red-shifts due to the carrier density change induced by the injected light. However, Fig. 3(a) shows that the shape of the modulation response is altered under injection-locking with an amplitude much weaker than in the free-running case.

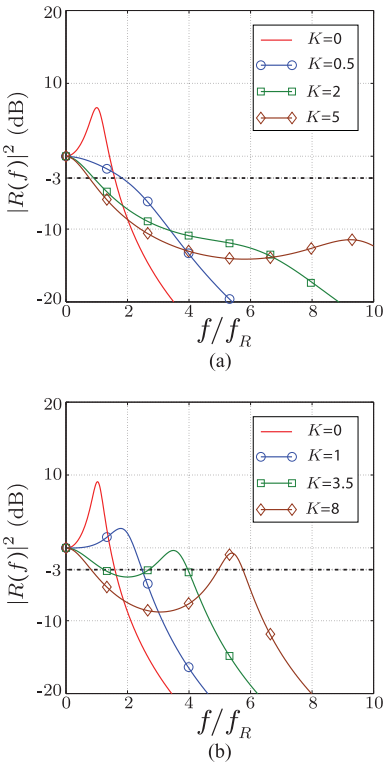


Fig. 3. Transfer functions calculated from (9) for the sole OIL laser ($g = 1$) and (a) $\gamma_b = 12$ GHz and $K = \{0, 0.5, 2, 5\}$, with corresponding $\Delta f/f_R = \{0, -2.20, 1.12, 6.10\}$, and (b) $\gamma_b = 20$ GHz and $K = \{0, 1, 3.5, 8\}$, with corresponding $\Delta f/f_R = \{0, -0.6, 1.7, 4.0\}$.

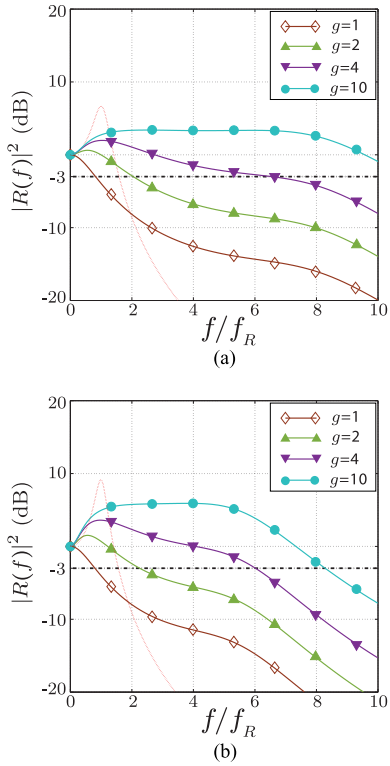


Fig. 4. Transfer functions calculated from (9) for the OILGL laser for $g = \{1, 2, 4, 10\}$ with (a) $\gamma_b = 12$ GHz, $K = 4$, $\Delta f/f_R = 1.5$, and (b) $\gamma_b = 20$ GHz, $K = 10$, $\Delta f/f_R = 0.5$.

Fig. 3(b) shows transfer functions obtained for a value of $\gamma_b$ of 20 GHz, in which case the relaxation oscillations of the solitary laser have a frequency of 8 GHz and appear as a stronger peak in the transfer function. Calculations are done with $K = 0$, 1, 3.5, 8, while the corresponding values of the normalized detuning are set to $\Delta f/f_R = 0$, $-0.6$, 1.7, 4.0. Note that this value of $\gamma_b$ is closer to that reported for QD lasers under normal operation, but as gain compression is not taken into account in the present model the value of $f_R$ may be slightly overestimated [35]–[37]. This case better reveals the evolution of the transfer function of an optically injection-locked laser: as the injection becomes stronger, while the resonance is pushed towards higher frequencies due to the red-shift of the SL, a dip appears at lower frequencies and limits the $-3$ dB bandwidth. The behavior is thus complementary to that of the free-running GL laser, where the relaxation oscillation frequency did not change while the modulation efficiency was strongly increased. It can be seen that $f_{-3dB}$ would also largely increase, and reach almost $6\times f_R$ for $K = 8$, if the dip was not appearing in the transfer function as injection becomes stronger. These simulations give an account of the well-known fact that when using solely optical injection, while large values of $K$ are required to push the resonance frequency towards higher values, the $-3$ dB bandwidth may then not significantly increase or may even be reduced due to the pre-resonance frequency dip [26]. For instance, Fig. 3(b) shows that for ($K = 8$, $\Delta f/f_R = 4$), the dip crosses the $-3$ dB line and in fact reduces by half the $-3$ dB modulation bandwidth. As a conclusion, although the largest values of $f_R$ can be obtained under strong optical injection, the corresponding modulation bandwidth is significantly reduced making sole optically injection-locked DMLs unsuitable for broadband applications.

### C. Combined Effects

From the results presented above, it can be anticipated that the drawbacks of both effects may be able to balance each other: while optical injection allows reaching high relaxation oscillation frequencies with weak modulation efficiency, the GL effect allows greatly increasing the modulation efficiency with little effect on the resonance frequency. Fig. 4 show situations where GL and optical injection are used simultaneously for the two values of $\gamma_b$ studied. The red line represents the transfer function in the free-running case under uniform pumping conditions ($K = 0, \phi = -\pi/2$, and $g = 1$). The other lines are obtained by fixing the injection-locking conditions $\{K, \Delta f/f_R\}$ to $\{4, 1.5\}$ for the case $\gamma_b = 12$ GHz and $\{10, 0.5\}$ for the case $\gamma_b = 20$ GHz, while $g$ is varied from 1 (no GL effect) to 10 (strong asymmetry in the pumping). Here, the values of $\Delta f/f_R$ were chosen so that the SL is operated inside the locking range, away from the Hopf bifurcation, in order to obtain a flat modulation response. When the GL is raised ($g = 2, 4, 10$), simulations show that the undesirable dip observed in the modulation response is lifted up without sacrificing the high resonance frequency. For instance, for $g = 4$, the pre-resonance dip is lifted towards the $-3$ dB level, allowing recovery of the modulation bandwidth. The most promising result is obtained with $g = 10$: in this case,

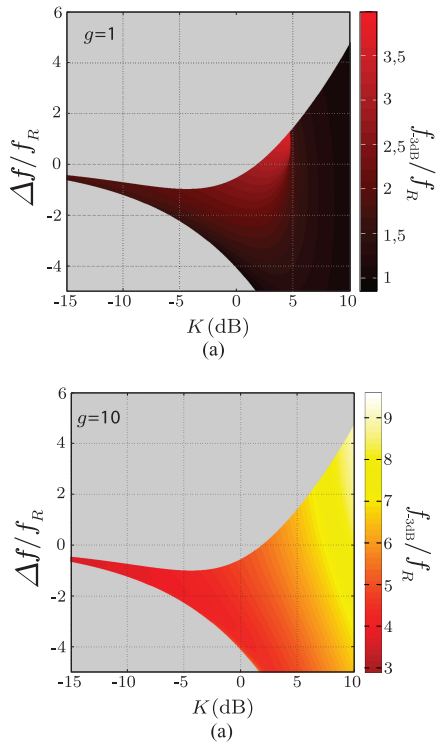


Fig. 5. $f_{-3\mathrm{dB}}/f_{\mathrm{R}}$ in the stable-locking region of the OILGL laser with $\gamma_{\mathrm{b}} = 20$ GHz, for (a) $g = 1$ and (b) $g = 10$. Areas in grey are outside the stable-locking region.

the coupled oscillator can reach $-3$ dB modulation bandwidths as large as $10 \times f_{\mathrm{R}}$. However, a large GL effect may not always be suitable for practical applications as there may be a tradeoff between modulation bandwidth and modulation efficiency, as strong levels of the latter may not be tolerable in many digital applications [38]. It can however be seen that very flat modulation response can be achieved by operating the SL away from the boundaries of the locking region, where the resonance peak would be much stronger. Finally, the results depicted in Fig. 4(a) and (b) are found in a qualitative agreement with the only experimental results published in the literature with an OILGL laser [29]. In order to understand the effect of GL within the whole stable-locking region, maps of the bandwidth of the optically injection-locked laser for various injection conditions are presented in Fig. 5 for $\gamma_{\mathrm{b}} = 20$ GHz, with and without GL. The maps reveal that for a laser with $f_{\mathrm{R}} = 8$ GHz, while optical injection alone allows for $-3$ dB bandwidths of at most 32 GHz ($4\times f_{\mathrm{R}}$), the GL effect allows reaching bandwidths above 60 GHz ($g = 10$) within reasonable optical injection conditions. It can be seen in Fig. 5(a) that in the upper part of the map and for values of $K$ close to 5 dB, $f_{-3\mathrm{dB}}$ suddenly drops from $4 \times f_{\mathrm{R}}$ to values below $f_{\mathrm{R}}$. This corresponds to the situation where the dip in the transfer function crosses the $-3$ dB line, as depicted in Fig. 4(b). When the GL is used, a substantial enhancement of the modulation dynamics is observed. In Fig. 5(b), the injection-locking map calculated for $g = 10$ allows identifying operating positions where the modulation bandwidth can be well above 40 GHz. These results are of prime importance for the development of novel DML transmitters operating at 40 Gb/s and beyond.

## IV. Conclusion

This paper theorizes for the first time the concept of the OILGL laser using small-signal analysis of a set of differential rate equations. Following a semi-analytical approach, a novel formulation of the modulation transfer function is derived. In addition, calculations show that an injection-locked GL-laser constitutes a powerful technique to increase the resonance frequency of the DML and greatly improving its $-3$ dB bandwidth, making it possible to reach values above 60 GHz using a laser with relaxation oscillations between 4 and 8 GHz and without modulation of the injected light. Future work will concentrate on the incorporation of the fine structure of QD nanostructures into the rate equations, on the experimental demonstration of the enhanced modulation dynamics of OILGL lasers as well as on the study of the impact of OIL on the frequency chirp of the GL laser. These results are of prime importance for low-cost applications including the development of high-bandwidth directly-modulated optical sources for future high-speed optical networks as well as monolithic integrated injection-locked laser networks with SLs referenced to the same ML.

## Acknowledgment

The authors would like to thank Prof. M. Osinski from the University of New-Mexico, USA, for fruitful discussions.

## References

[1] T. Yamamoto, "High-speed directly modulated lasers," in *Proc. Opt. Fiber Commun. Conf.*, Mar. 2012, pp. 225–228, Paper OTh3F.
[2] C.-H. Lee, *Microwave Photonics*. Boca Raton, FL, USA: CRC Press, 2007.
[3] L. A. Coldren and S. W. Corzine, *Diode Lasers and Photonic Integrated Circuits*, New York, NY, USA: Wiley-Interscience, 1995.
[4] D. Erasme *et al.*, "The dual-electroabsorption modulated laser, a flexible solution for amplified and dispersion uncompensated networks over standard fiber," *J. Lightw. Technol.*, vol. 32, no. 21, pp. 4068–4078, Sep. 2014.
[5] R. S. Tucker, "Green optical communications Part II: Energy limitations in networks," *IEEE J. Sel. Topics Quantum Electron.*, vol. 17, no. 2, pp. 261–274, Mar. 2011.
[6] E. Murphy, "The semiconductor laser: Enabling optical communication," *Nature Photon.*, vol. 4, no. 10, p. 287, May 2014.
[7] A. Frommer, S. Luryi, D. Nichols, J. Lopata, and W. Hobson, "Direct modulation and optical confinement factor modulation of semiconductor lasers," *Appl. Phys. Lett.*, vol. 67, no. 12, pp. 1645–1647, Sep 1995.
[8] K. Nakahara *et al.*, "High extinction ratio operation at 40 Gb/s direct modulation in 1.3-$\mu$m InGaAlAs-MQW RWG DFB lasers," presented at the Opt. Fiber Commun. Conf., Anaheim, CA, USA, 2006.
[9] S. Weisser *et al.*, "Damping-limited modulation bandwidths up to 40 GHz in undoped short-cavity $In_{0.35}Ga_{0.65}As$-GaAs multiple-quantum well lasers," *IEEE Photon. Technol. Lett.*, vol. 8, no. 5, pp. 608–610, May 1996.
[10] N. Suzuki *et al.*, "25 Gbps operation of 1.1 $\mu$m-range InGaAs VCSELs for high-speed optical interconnections," presented at the Opt. Fiber Commun. Conf., Anaheim, CA, USA, 2006.
[11] W. Hofmann *et al.*, "10 Gb/s data transmission using BCB passivated 1.55 $\mu$m InGaAlAs-InP VCSELs," *IEEE Photon. Technol. Lett.*, vol. 18, no. 2, pp. 424–426, May 2006.
[12] T. B. Simpson, J. Liu, and A. Gavrielides, "Bandwidth enhancement and broadband noise reduction in injection-locked semiconductor lasers," *IEEE Photon. Technol. Lett.*, vol. 7, no. 7, pp. 709–711, Jul. 1995.
[13] E. K. Lau *et al.*, "Strong optical injection-locked semiconductor lasers demonstrating $>$ 100-GHz resonance frequencies and 80-GHz intrinsic bandwidths," *Opt. Exp.*, vol. 16, no. 9, pp. 6609–6618, Apr. 2008.
[14] K. Y. Lau, "Gain-levered semiconductor laser direct modulation with enhanced frequency modulation and suppressed intensity modulation," *IEEE Photon. Technol. Lett.*, vol. 3, no. 8, pp. 703–705, Aug. 1991.

[15] K. Vahala, M. A. Newkirk, and T. Chen, "The optical gain lever: A novel gain mechanism in the direct modulation of quantum well semiconductor lasers," *Appl. Phys. Lett.*, vol. 54, no. 25, pp. 2506–2508, Jun. 1989.

[16] F. Mogensen, H. Olesen, and G. Jacobsen, "Locking conditions and stability properties of a semiconductor laser with external light injection," *IEEE J. Quantum Electron.*, vol. 21, no. 7, pp. 784–793, Jul. 1985.

[17] L. E. Erikson and A. Szabo, "Spectral narrowing of dye laser output by injection of monochromatic radiation into the laser cavity," *Appl. Phys. Lett.*, vol. 18, no. 10, pp. 433–435, Oct 1971.

[18] F. Mogensen, H. Olesen, and G. Jacobsen, "Optical FM signal amplification and FM noise reduction in an injection locked AlGaAs semiconductor laser," *Electron. Lett.*, vol. 16, no. 21, pp. 696–697, Jul. 1985.

[19] T. Kobayashi, Y. Yamamoto, and T. Kimura, "Optical FM signal amplification and FM noise reduction in an injection locked AlGaAs semiconductor laser," *Electron. Lett.*, vol. 17, no. 22, pp. 849–851, Oct. 1981.

[20] C. Lin and F. Mengel, "Reduction of frequency chirping and dynamic linewidth in high speed directly modulated semiconductor lasers," *Electron. Lett.*, vol. 20, no. 25, pp. 1073–1075, Dec. 1984.

[21] P. Gallion, H. Nakajima, G. Debarge, and C. Chabran, "Contribution of spontaneous emission to the linewidth of an injected-locked semiconductor laser," *Electron. Lett.*, vol. 21, no. 14, pp. 626–628, Jul. 1995.

[22] L. Chrostowski *et al.*, "40 GHz bandwidth and 64 GHz resonance frequency in injection-locked 1.55 $\mu$m VCSELs," *IEEE J. Sel. Topics Quantum Electron.*, vol. 13, no. 5, pp. 1200–1208, Sep./Oct. 2007.

[23] N. Naderi *et al.*, "Modeling the injection-locked behavior of a quantum dash semiconductor laser," *IEEE J. Sel. Topics Quantum Electron.*, vol. 15, no. 3, pp. 563–571, May 2009.

[24] L. F. Lester, N. A. Naderi, F. Grillot, R. Raghunathan, and V. Kovanis, "Strong optical injection and the differential gain in a quantum dash laser, optics express," *Opt. Exp.*, vol. 22, no. 6, pp. 7222–7228, Mar. 2014.

[25] N. Moore and K. Lau, "Ultrahigh efficiency microwave signal transmission using tandem contact single quantum well GaAlAs lasers," *Appl. Phys. Lett.*, vol. 55, no. 10, pp. 936–938, Sep. 1989.

[26] D. Gajic and K. Y. Lau, "Intensity noise in the ultrahigh efficiency tandem-contact quantum well lasers," *Appl. Phys. Lett.*, vol. 57, no. 18, pp. 1837–1839, Oct. 1990.

[27] Y. Li, N. Naderi, V. Kovanis, and L. Lester, "Enhancing the 3-dB bandwidth via the gain-lever effect in quantum-dot lasers," *IEEE Photon. J.*, vol. 2, no. 3, pp. 321–329, Jun. 2010.

[28] M. Pochet, N. G. Usechak, J. Schmidt, and L. F. Lester, "Modulation response of a long-cavity, gain-levered quantum-dot semiconductor laser," *Opt. Exp.*, vol. 22, pp. 1726–1734, 2014.

[29] H.-K. Sung, T. Jung, D. Tishinin, K.-Y. Liou, W. Tsang, and M. Wu, "Optical injection-locked gain-lever distributed Bragg reflector lasers with enhanced RF performance," in *Proc. IEEE Microw. Photon., Int. Top. Meet.*, Oct. 2004, pp. 225–228.

[30] A. Gavrielides, V. Kovanis, and T. Erneux, "Analytical stability boundaries for a semiconductor laser subject to optical injection," *Opt. Commun.*, vol. 136, nos. 3/4, pp. 253–256, Apr. 1997.

[31] N. A. Naderi, "Quantum dot gain-lever laser diode," M.S. thesis, Univ. of New Mexico, Albuquerque, NM, USA.

[32] X. Jin and S.-L. Chuang, "Bandwidth enhancement of Fabry-Perot quantum-well lasers by injection-locking," *Solid-State Electron.*, vol. 50, no. 6, pp. 1141–1149, Jun. 2006.

[33] C. Wang, F. Grillot, and J. Even, "Impacts of wetting layer and excited state on the modulation response of quantum-dot lasers," *IEEE J. Quantum Electron.*, vol. 48, no. 9, pp. 1144–1150, Sep. 2012.

[34] F. Grillot, C. Wang, N. A. Naderi, and J. Even, "Modulation properties of self-injected quantum-dot semiconductor diode lasers," *IEEE J. Sel. Topics Quantum Electron.*, vol. 19, no. 4, art. no. 1900812, Jul./Aug. 2013.

[35] F. Grillot, B. Dagens, J. G. Provost, H. Su, and L. F. Lester, "Gain compression and above-threshold linewidth enhancement factor in 1.3-m InAs-GaAs quantum-dot lasers," *IEEE J. Quantum Electron.*, vol. 44, no. 10, pp. 946–951, Oct. 2008.

[36] M. T. Crowley, N. A. Naderi, H. Su, F. Grillot, and L. F. Lester, "GaAs based quantum dot lasers," in *Semiconductors Semimetals: Advances Semiconductor Lasers*, vol. 86. New York, NY, USA: Academic, ch. 10, pp. 371–417, May 2012.

[37] C. Otto, K. Luedge, E. Viktorov, and T. Erneux, "Quantum dot laser tolerance to optical feedback," in *Nonlinear Laser Dynamics: From Quantum Dots to Cryptography*. Weinheim, Germany: Wiley-VCH, Dec. 2011, ch. 2, pp. 139–158.

[38] X. Zhao, L. Chrostowski, and C. H. Hasnain, "High extinction ratio of injection-locked VCSELs," *IEEE Photon. Technol. Lett.*, vol. 18, no. 1, pp. 166–168, Jan. 2006.


**Jean-Maxime Sarraute** was born in Marseille, France, in 1989. He received the M.Sc. degree from the Engineering School, Telecom Paristech, Paris, France, in 2014. He is currently working toward the Ph.D. degree at the Communications and Electronic Department, Telecom Paristech, and with the Optical Center, Photonic and Laser, Qubec, QC, Canada.

His current research interests include modeling microring and quantum dots lasers.

**Kevin Schires** received the Diplme d'Ingnieur degree in signal processing and telecommunications from the cole Suprieure d'Ingnieurs en lectronique et lectrotechnique, Paris, France, and the Ph.D. degree in semiconductor electronics from the University of Essex, Colchester, U.K.

He is currently a Postdoctoral Researcher at the Communications and Electronic Department, Telecom Paristech (alias Ecole Nationale Suprieure des Tlcommunications), Paris.

**Sophie LaRochelle** (M'00–SM'13) received the bachelor's degree in engineering physics from Universit Laval, Qubec, QC, Canada, in 1987, and the Ph.D. degree in optics from the University of Arizona, Tucson, AZ, USA, in 1992.

From 1992 to 1996, she was a Research Scientist with the Defense Research and Development Canada, Valcartier, where she worked on electrooptical systems. She is currently a Professor at the Department of Electrical and Computer Engineering, Universit Laval, where she holds a Canada Research Chair (Tier 1) in Advanced Photonics Technologies for Communications. Her current research interests include active and passive components for optical communication systems including silicon photonic devices, Bragg gratings filters, multiwavelength, and pulsed fiber lasers. Other research interests include optical fibers and amplifiers for spatial division multiplexing, all-optical signal processing and routing, and transmission of radio-over-fiber signals, including UWB and GPS.

Dr. LaRochelle is an OSA Fellow.

**Frédéric Grillot** (SM'12) was born in Versailles, France, on August 22, 1974. He received the M.Sc. degree from the University of Dijon, Dijon, France, in 1999, and the Ph.D. degree from the University of Besancon, Besancon, France, in 2003.

From 2003 to 2004, he was with the Institut d'Electronique Fondamentale, University Paris-Sud, where he focused on integrated optics modelling and on Si-based passive devices for optical interconnects. From 2008 to 2009, he was also a Visiting Professor at the Center for High Technology Materials, University of New-Mexico, USA, where his research interest includes optoelectronics. Since September 2004, he has been with the Institut National des Sciences Appliques, Lyon, France, as an Associate Professor. Since October 2012, he has been an Associate Professor at the Communications and Electronic Department, Telecom Paristech (alias Ecole Nationale Suprieure des Tlcommunications), Paris, France. He is the Author or Coauthor of 61 journal papers, one book, two book chapters, and more than 140 contributions in international conferences and workshops. His doctoral research interests were conducted within the Optical Component Research Department, Alcatel-Lucent, which include the effects of the optical feedback in semiconductor lasers, and the impact this phenomenon has on optical communication systems. His current research interests include advanced laser diodes using new materials including quantum dots and dashes for low-cost applications, nonlinear dynamics, and optical chaos in semiconductor lasers systems, as well as microwave and silicon photonics applications including photonic clocks and photonic analog to digital converters.

Dr. Grillot is an Associate Editor for *Optics Express*, a Senior Member of the SPIE and of the IEEE Photonics Society, as well as a Member of the OSA.